Transtemporal Ultrasound Holograms for Thalamic Therapy

Diana Andrés, Noé Jiménez, Francisco Camarena
Instituto de Instrumentación para Imagen Molecular, Universitat Politècnica de València, Spain
Email: diaanbau@upv.es

***Abstract*—In this work, we numerically investigate the performance of acoustic holograms at 650 kHz to correct the aberrations introduced by the skull and simultaneously target the thalamic nuclei through the temporal bone window. The influence of a misalignment in the skull-lens relative location is also studied in terms of focus pressure and treated volume. For five different holograms we have seen an improvement on the sonicated target volume compared to the sonicated healthy brain tissue, from 1.5 to 9.5 times better than with a focused transducer. For alignment errors in the skull-lens relative position lower than 3.75 degrees of rotation the hologram produces a field with a peak pressure higher that -1 dB the maximum pressure in the correct position. We demonstrate that transtemporal acoustic holograms are a robust method to improve focus quality and to enhance sonicated volumes on target deep-brain even under small misallocations of the therapeutic ultrasound device that can be used for highly selective and low-cost blood-brain barrier opening and neuromodulation applications.**

***Index Terms*—Therapeutic ultrasound, neuromodulation, blood-brain barrier opening, acoustic holograms.**

I. Introduction

By nature, ultrasound can propagate through the skull and interact with the brain tissue, producing mechanical and thermal effects in a non-invasively and non-ionizing manner. These effects allow for local temperature raising, ranging from mild hyperthermia (40-45 °C) [1], used for drug delivery and chemotherapy enhancement [2], to thermal ablation (temperatures above 55 °C) [3]. On the other hand, at lower acoustical intensities mechanical effects can trigger neuromodulation [4] or blood-brain barrier opening [5], the latter effect widely used for drug and gene delivery in a localized and safe manner.

However, when focusing ultrasound on a non-invasive way, i.e., without surgical interventions, sound waves must break through the skull, which acts as a mechanical wall of great stiffness and complex internal structure; producing strong refraction and attenuating effects to the propagating sound wave. This results in an uncontrolled beam focusing that might sonicate out-of-target brain structures. To overcome this, MRI-guided phased-array systems have emerged as the gold-standard for transcranial ultrasound applications [6] due to the precise phase and amplitude control, which enables the compensation of the aberrations by actively time-delaying the ultrasound signals, and monitoring the treatment using MRI-Thermometry. Unfortunately, this is a high-cost an complex technology, not available for all medical facilities. Recently, 3D-printed lenses were reported as a low-cost alternative for skull aberration correction for fixed [7], or mechanically steered target locations [8]. This approach was enhanced by using acoustic holograms to match the focus shape and size to those of the therapeutic target [9] and to create bilateral focusing at deep-brain structures [10], or even vortex beams [11].

In this work, we propose ultrasound holograms adapted to the temporal bone window, which is the thinnest part of the human skull and is usually used for brain imaging [12]. Using this window, we can tackle deep-brain bilateral targets while attenuation and skull heating is minimized. In addition, it is not mandatory to shave the head of the patient, which might be a concern for recursive treatments such as neuromodulation and long drug delivery therapies. In particular, we study numerically the transtemporal focalization using a focused transducer on both thalamic nuclei, deep-brain targets of great neurological interest [13]. Five different holographic lenses coupled to a flat transducer have also been studied and compared with the performance of the single element focused transducer in terms of skull aberration correction and optimization of the thalamic volume sonicated. In addition, we report the robustness of acoustic holograms under small misallocations between the skull and the ultrasound transducer.

II. Materials and Methods

A flat circular transducer of 65 mm-aperture located at 15 mm from the skin was located in front of the temporal bone window. This arrangement allows for a good coupling between the holographic lenses and the flat transducer, ensuring the lens is not in direct contact with the skull. A focused transducer with the same aperture and radius of curvature $F = 80$ mm, located in the same position and at 13 mm from the skull has been used to compare focusing quality and treated volumes. Both transducers have a central frequency of 650 kHz.

To create acoustic holograms inside the skull and following the shape of the thalamus, we first acquire tomographic MRI data for soft tissue segmentation and x-ray CT images to extract bone properties. A skull from an anonymous

2021 IEEE International Ultrasonics Symposium (IUS) | 978-1-6654-0355-9/21/$31.00 ©2021 IEEE | DOI: 10.1109/IUS52206.2021.9593685

978-0-7381-1209-1/21/$31.00 ©2021 IEEE

Authorized licensed use limited to: UNIVERSIDAD POLITECNICA DE VALENCIA. Downloaded on November 30,2021 at 13:55:12 UTC from IEEE Xplore. Restrictions apply.

patient in this study was used, whose CT images were obtained using a GE LightSpeed VCT 64 scanner (GE Medical Systems, Milwaukee, WI) at 0.49 mm × 0.48 mm × 0.63 mm resolution. Hounsfield units obtained were converted to density and sound speed maps using empirical linear fits [14], resulting mean values of $\rho_s = 1611$ kg/m^3, and $c_s = 2333$ m/s, for the density and sound speed in the bones, respectively. Acoustic attenuation was considered constant for all skull, with a value of $\alpha_s = 8.37$ dB/(cm·MHz$^\gamma$), $\gamma = 1.1$, according to the literature [15]. Brain was supposed as a homogeneous media inside the skull with density $\rho_b = 1000$ kg/m^3, sound speed $c_b = 1560$ m/s and attenuation $\alpha_b = 0.66$ dB/(cm·MHz$^\gamma$), values obtained from literature [16]. Thalamus segmentation was obtained from an MRI extracted from the open-access human atlas of the International Consortium for Brain Mapping (ICBM) from the Laboratory of Neuro Imaging [17]. Total brain and both thalami volumes are 1523 cm^3 and 7.9 cm^3, respectively.

Acoustic holograms were designed using time-domain pseudo-spectral simulations with the k-Wave software [18] and a phase-conjugation method with virtual sources, as described previously in Ref. [9]. Five different configurations of the virtual sources were studied and compared of the propagated field produced by the curved transducer inside the brain: a point hologram between both thalamic nuclei, Fig. 1(b), a line hologram, a bifocal point hologram in the middle of each nucleus, a bifocal line hologram, Fig. 1 (c), and a bifocal plane hologram. The wavefront produced by the virtual sources is recorded in a plane parallel to the transducer surface and the lens is designed with the phase – conjugated information, considering that each pixel of the lens vibrates as an elastic Fabry-Perot resonator. Each pixel has a size of 0.39 x 0.39 mm2, having a total of about 22000 elements, each one emitting a different sound waves and, therefore, acting as an element of a phased-array system. A scheme of the therapeutic system dimensions and location is shown in Fig. 1 (a).

Finally, we obtained the acoustic field produced by each lens-transducer system inside the brain with numerical simulations and considering the Clear resin (Formlabs) measured acoustic properties ($\rho_L = 1171$ kg/m^3, $c_L = 2580$ m/s and $\alpha_L = 2.87$ dB/(cm·MHz$^\gamma$), which were like those reported in the literature for similar photopolymers [19].

All simulations were done with a grid size of $\lambda/6$ = 0.39 mm in each dimension for a frequency of 650 kHz and water medium surrounding the skull. Both focused and flat transducers with holographic lenses were driven with a 100-cycles sinusoidal tone burst and acoustic pressure of 1 Pa at the transducer surface. Simulations were running for enough time (300 μs) to consider multiple reflections of the ultrasound inside the skull.

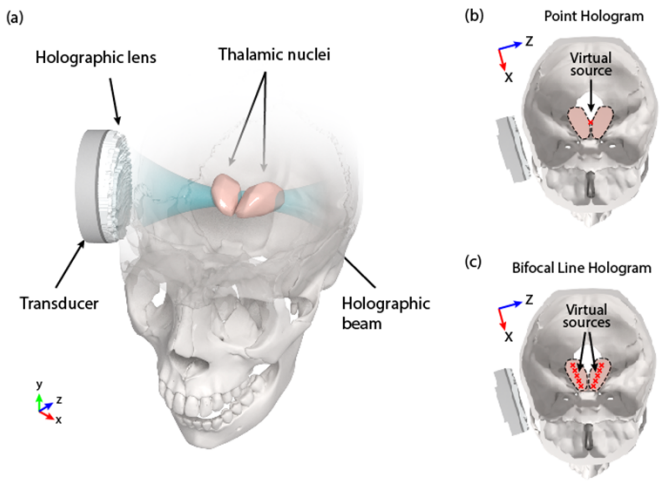


Fig. 1. a) Scheme of the transtemporal transducer-lens system for thalamic focusing. b) point hologram virtual source location. c) Bifocal line hologram virtual sources location.

III. Results

For finite-amplitude waves, and when all emitters are active, both beams interact and due to material and advective nonlinearity wave mixing occurs during On the one hand, the ultrasound beam produced by the reference focused transducer was simulated. The focal spot presents strong aberrations, even the transducer was aligned with the temporal bone window for normal incidence of the acoustic waves. Maximum pressure gain of the focus inside the skull is 4.7 p/p_0, where p_0 is the pressure at the transducer surface. Considering sonicated volumes as those with a pressure higher than -3 dB the maximum value, we obtained that 0.28 cm^3 (3.6%) of the thalamus volume is covered with one sonication, while 1.21 cm^3 of the brain outside the target were treated. The ratio between the sonicated thalamic and non-thalamic volumes is 0.23.

On the other hand, the abovementioned five different holograms were simulated. For both one-point and one-line holograms, pressure gains, defined as half the average pressure at the exit plane of the holographic lens, are 7.6 p/p_0 and 5.9 p/p_0. With the same -3 dB threshold, 5.2% and 8.5% of both therapeutic targets is sonicated with these holograms, respectively, while the sonicated non-target brain volume is 0.19 cm^3 and 0.77 cm^3. For these holograms, the thalamic-brain sonicated ratios are 2.16 and 0.88, showing an improvement with respect to the curved transducer field of 9.4 and 3.8 times for the point and lines holograms, respectively. Also, pressure gain on the focal region is better since the corresponding energy is concentrated in the focal spot and no aberrations or lateral lobes are produced. Similar results were obtained for the three holograms designed for bifocal targeting. For the two-point hologram, 4.5% of the target structure has been treated, while 0.45 cm^3 of the brain is sonicated, with pressure gain of 5.8 p/p_0

Authorized licensed use limited to: UNIVERSIDAD POLITECNICA DE VALENCIA. Downloaded on November 30,2021 at 13:55:12 UTC from IEEE Xplore. Restrictions apply.

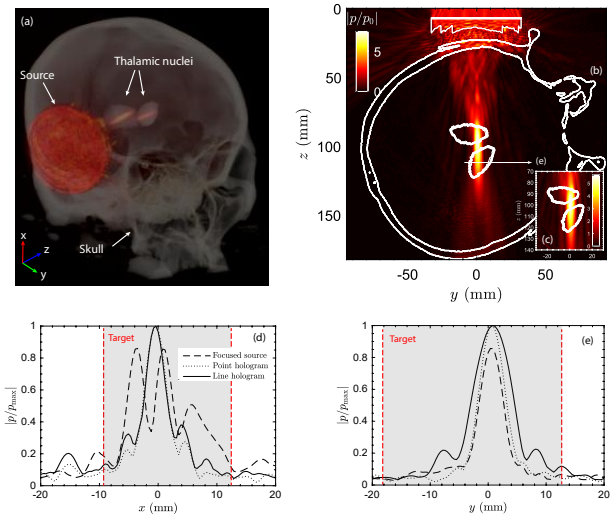


Fig. 2. a) 3D representation of bifocal sonication with two-points hologram. b) Coronal cut of the point hologram and (c) line hologram. d) Normalized pressure comparison in a cut along the y-axis. e) Normalized pressure comparison in a cut along the x-axis.

and 3.7 p/p_0 at right and left thalami, respectively. In the two-lines hologram we get to treat 17.1% of both thalami in one sonication, sonicating 4.94 cm^3 of the brain with pressure gain of 3.9 p/p_0 and 3.4 p/p_0 at right and left thalami, respectively. With the two-planes hologram, we treat 15.3% of both therapeutic targets while sonicating 5.84 cm^3 of the non-target brain tissue with pressure gain of 3.4 p/p_0 and 3.3 p/p_0 at left and right thalami, respectively.

Finally, a set of simulations were performed to study how a misallocation of the transducer-lens system relative to the target position could affect the focusing capabilities, in terms of pressure gain at the focal point and thalamic and brain sonicated volumes. The results are summarized in Fig. 3. Performance of the one line, two points and two planes hologram have been studied for rotation errors of 1.25° from 0° to 17.5°. Normalized peak pressure is calculated as the pressure gain relative to the pressure at the transducer surface and to half the average pressure at the exit of the holographic lens for the focused transducer and holograms, respectively. Volumes are calculated as the region with a pressure gain between the maximum and -3 dB for each focus separately.

For the curved transducer, its focus quality does not change under rotation from the center of the skull. The main change in sonicated volumes and peak pressures is due to the secondary lobes that appear due to the aberrations introduced by the skull. The maximum change in pressure values is 8% of the original pressure gain, and sonicated volumes of the brain and both thalami remain almost constant.

For the line hologram, the maximum pressure decreases with the rotated angle and treated volumes increase, which means that the hologram loses resolution when it is not correctly positioned. At 17.5° of rotation, the acoustic pressure at the focus is reduced by 32% of the original value and the volume outside the target is 8.3 times greater. Also, the target volume covered is increased 1.5 times compared to the original location. For rotation angles below 5° both volumes outside and inside the target remain almost constant (below 10% of increase) while the difference of pressure gain is 15%.

In the case of the two-point configuration, right focus presents more pressure amplitude and has a more delimited shape. While rotating the lens around the skull, for an error of 5° the loss in pressure at the right focus location is 21%, and for 17.5° this loss arrives at 52%. Thalamic volume covered is increased 1.2 times while sonicated volume outside the target is 2.7 times greater for 5° of rotation error. This proportions are 4.7 and 29.7 times greater when the rotation error is 17.5°, respectively. Note that using the two-plane hologram both foci are wider than in the two-point hologram, meaning that the same energy is distributed in a wider area. Therefore, under small rotation errors the pressure gain is smaller and the focus shape becomes partially blurred, as can be observed in Fig. 3. Pressure gain barely decreases, but sonicated volumes rapidly increase because greater volumes are sonicated with the same energy.

IV. Conclusions

The results of this study prove that acoustic holograms could improve sonication through the transtemporal bone window. The results show that the thalamic treated volume is optimized in all the cases, reducing the amount of energy outside the target. Also, using holograms the pressure gain is higher since the aberrations introduced by the skull are corrected, and no side lobes appear at the focal region. In addition, the parametric study showed that the performance of holographic lenses under a rotation error lesser than 5° are pretty good, which shows the great stability of these systems. In this sense, transtemporal acoustic holograms are a robust method to improve focus quality and to enhance sonicated volumes on deep-brain targets even under small misallocations of the therapeutic ultrasound device. The temporal window is especially important for small-aperture holograms, when all energy propagates through a small portion of skull and could overheat it locally. This technology might be used for highly selective and low-cost blood-brain barrier opening, neuromodulation or hyperthermia applications.

V. Acknowledgments

This research has been supported by the Spanish Ministry of Science, Innovation and Universities (MICINN) through grants IJC2018-037897-I, FPU19/00601 and PID2019-111436RB-C22, by the Agència Valenciana de la Innovació through grants INNCON/2021/8 and INNVA1/2020/92, by Generalitat Valenciana through grant AICO/2020/268. Action co-financed

Authorized licensed use limited to: UNIVERSIDAD POLITECNICA DE VALENCIA. Downloaded on November 30,2021 at 13:55:12 UTC from IEEE Xplore. Restrictions apply.

by the European Union through the Programa Operativo del Fondo Europeo de Desarrollo Regional (FEDER) of the Comunitat Valenciana 2014-2020 (IDIFEDER/2018/022) and (IDIFEDER/2021/004).

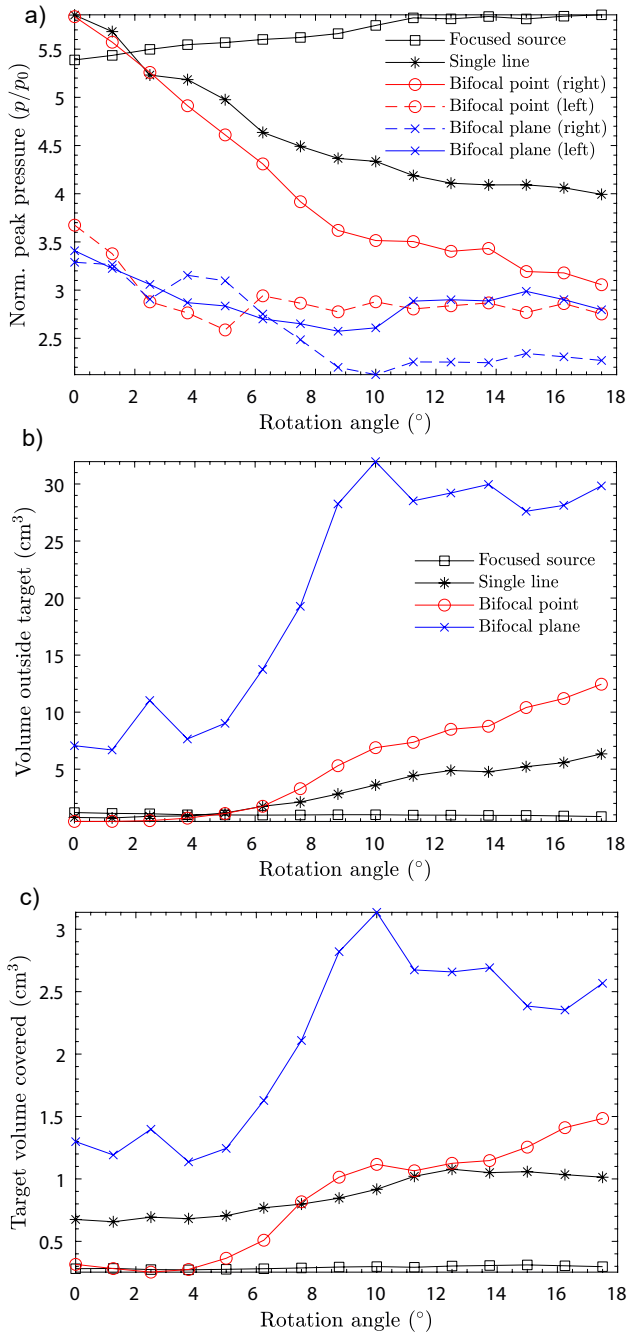


Fig. 3. Parametric study depending on the skull rotated angle. a) Maximum pressure at focus. b) Sonicated volume outside the therapeutic target, in the brain. c) Sonicated organ volume.

REFERENCES

[1] M. Tillander, S. Hokland, J. Koskela, H. Dam, N. P. Andersen, M. Pedersen, K. Tanderup, M. Ylihautala, and M. Köhler, "High intensity focused ultrasound induced in vivo large volume hyperthermia under 3d mri temperature control," 2016.

[2] M. D. Gray, P. C. Lyon, C. Mannaris, L. K. Folkes, M. Stratford, L. Campo, D. Y. Chung, S. Scott, M. Anderson, R. Goldin, *et al.*, "Focused ultrasound hyperthermia for targeted drug release from thermosensitive liposomes: results from a phase i trial," *Radiology*, vol. 291, no. 1, pp. 232–238, 2019.

[3] D. Coluccia, J. Fandino, L. Schwyzer, R. O?Gorman, L. Remonda, J. Anon, E. Martin, and B. Werner, "First noninvasive thermal ablation of a brain tumor with mr-guided focusedultrasound," *Journal of therapeutic ultrasound*, vol. 2, no. 1, pp. 1–7, 2014.

[4] J. Blackmore, S. Shrivastava, J. Sallet, C. R. Butler, and R. O. Cleveland, "Ultrasound neuromodulation: a review of results, mechanisms and safety," *Ultrasound in medicine & biology*, vol. 45, no. 7, pp. 1509–1536, 2019.

[5] A. N. Pouliopoulos, S.-Y. Wu, M. T. Burgess, M. E. Karakatsani, H. A. Kamimura, and E. E. Konofagou, "A clinical system for non-invasive blood–brain barrier opening using a neuronavigation-guided single-element focused ultrasound transducer," *Ultrasound in medicine & biology*, vol. 46, no. 1, pp. 73–89, 2020.

[6] N. Lipsman, Y. Meng, A. J. Bethune, Y. Huang, B. Lam, M. Masellis, N. Herrmann, C. Heyn, I. Aubert, A. Boutet, *et al.*, "Blood–brain barrier opening in alzheimer?s disease using mr-guided focused ultrasound," *Nature communications*, vol. 9, no. 1, pp. 1–8, 2018.

[7] G. Maimbourg, A. Houdouin, T. Deffieux, M. Tanter, and J.-F. Aubry, "3d-printed adaptive acoustic lens as a disruptive technology for transcranial ultrasound therapy using single-element transducers," *Physics in Medicine & Biology*, vol. 63, no. 2, p. 025026, 2018.

[8] G. Maimbourg, A. Houdouin, T. Deffieux, M. Tanter, and J.-F. Aubry, "Steering capabilities of an acoustic lens for transcranial therapy: numerical and experimental studies," *IEEE Transactions on Biomedical Engineering*, vol. 67, no. 1, pp. 27–37, 2019.

[9] S. Jiménez-Gambín, N. Jiménez, J. M. Benlloch, and F. Camarena, "Holograms to focus arbitrary ultrasonic fields through the skull," *Physical Review Applied*, vol. 12, no. 1, p. 014016, 2019.

[10] D. Andrés, S. Jiménez-Gambín, N. Jiménez, and F. Camarena, "Multifocal acoustic holograms for deep-brain neuromodulation and bbb opening," in *2020 IEEE International Ultrasonics Symposium (IUS)*, pp. 1–3, IEEE, 2020.

[11] S. Jiménez-Gambín, N. Jiménez, and F. Camarena, "Transcranial focusing of ultrasonic vortices by acoustic holograms," *Physical Review Applied*, vol. 14, no. 5, p. 054070, 2020.

[12] S. Purkayastha and F. Sorond, "Transcranial doppler ultrasound: technique and application," in *Seminars in neurology*, vol. 32, pp. 411–420, Thieme Medical Publishers, 2012.

[13] J. Chien, J. Cheng, and F. Lenz, "The thalamus," in *Conn's Translational Neuroscience*, pp. 289–297, Elsevier, 2017.

[14] T. D. Mast, "Empirical relationships between acoustic parameters in human soft tissues," *Acoustics Research Letters Online*, vol. 1, no. 2, pp. 37–42, 2000.

[15] R. S. Cobbold, *Foundations of biomedical ultrasound*. Oxford university press, 2006.

[16] B. E. Hammer, "Physical properties of tissues," *Radiology*, vol. 181, no. 1, pp. 128–128, 1991.

[17] P. A. Yushkevich, J. Piven, H. C. Hazlett, R. G. Smith, S. Ho, J. C. Gee, and G. Gerig, "User-guided 3d active contour segmentation of anatomical structures: significantly improved efficiency and reliability," *Neuroimage*, vol. 31, no. 3, pp. 1116–1128, 2006.

[18] B. E. Treeby, J. Jaros, A. P. Rendell, and B. Cox, "Modeling nonlinear ultrasound propagation in heterogeneous media with power law absorption using ak-space pseudospectral method," *The Journal of the Acoustical Society of America*, vol. 131, no. 6, pp. 4324–4336, 2012.

[19] K. Melde, A. G. Mark, T. Qiu, and P. Fischer, "Holograms for acoustics," *Nature*, vol. 537, no. 7621, pp. 518–522, 2016.

Authorized licensed use limited to: UNIVERSIDAD POLITECNICA DE VALENCIA. Downloaded on November 30,2021 at 13:55:12 UTC from IEEE Xplore. Restrictions apply.